International Journal of Engineering Science 193 (2023) 103941

Contents lists available at ScienceDirect

International Journal of Engineering Science

journal homepage: www.elsevier.com/locate/ijengsci

General theory for plane extensible elastica with arbitrary undeformed shape

Alessandro Taloni [a,b], Daniele Vilone [c,d,*], Giuseppe Ruta [e]

[a] CNR – Consiglio Nazionale delle Ricerche, Istituto dei Sistemi Complessi, via dei Taurini 19, Roma, 00185, Italy
[b] Center for Complexity and Biosystems, Department of Physics, University of Milan, Via Giovanni Celoria 16, Milan, 20133, Italy
[c] Laboratory of Agent Based Social Simulation, Institute of Cognitive Science and Technology, CNR, via Palestro 32, Roma, 00185, Italy
[d] Grupo Interdisciplinar de Sistemas Complejos, Departamento de Matemáticas, Universidad Carlos III de Madrid, Leganés, Madrid, 28911, Spain
[e] Dipartimento di Ingegneria Strutturale e Geotecnica, Sapienza Università di Roma, Via Eudossiana 18, Roma, 00184, Italy

ARTICLE INFO

Keywords:
Elasticity
Neutral curve
Linear deformations

ABSTRACT

A general expression for the strain energy of a homogeneous, isotropic, plane extensible elastica with an arbitrary undeformed configuration is derived. This expression appears to be suitable for one-dimensional models of polymers or vesicles, the natural configuration of which is characterized by locally changing curvature. In a linear setting, we derive the macroscopic stress–strain relations, providing an universal criterion for the neutral curve location. In this respect, we further demonstrate that the neutral curve existence constitutes the fundamental requirement for the conformational dynamics of any inextensbile biological filament.

1. Introduction

The old theories of flexure were based on the assumption that the strain of rod-like elastica consists of extension and contraction of an arrangement of longitudinal filaments, oftenly dubbed fibers (Bernoulli, 1691; Euler, 1771, 1960). In this context, the reduction of the elastica problem to that of a one-dimensional line, in a state of plane strain (Michell, 1901), was naturally taken as the compelling point of view. By instance, Lagrange considers the three-dimensional elastica as a *fil flexible et en même temps extensible et contractible* (Lagrange, 1853). Yet, in Kirchoff's theory the three-dimensional deformation of a slender elastic rod is reduced to the bending deformation of a one-dimensional curve (Kirchhoff, 1859). Moreover, the theory of the bending and twisting of thin rods and wires was for a long time developed independently of the general three-dimensional equations of elasticity, by one-dimensional methods akin to those employed by Bernoulli and Euler (Love, 2013). However, the problem of which, among the fibers composing the elastica, was eligible to be taken as the representative curve, remained unsettled till the profound works of Parent and Coulomb. Already in 1695, Jacob Bernoulli had argued that the bending moment had to be taken, at each cross-section, with respect to the point where it intersects the *line of fulcra*, i.e. the line which does not suffer any extension nor contraction all along the deformation: the neutral fiber. If the tensions vary linearly over the rod rigid cross-section, the neutral line coincides with its central line. Although this fact was already known by Beeckman, Hooke, Huygens, Varignon and Mariotte (Euler, 1960; Timoshenko, 1983), it was only in 1713 that these observations took the mathematical form of the Parent criterion (Parent, 1713).

The issue of the existence and ensuing location of the neutral fiber, avoiding any specific elastic hypothesis about the law of variation of the tensions over the cross-section, remains today unjustly unattended by modern scientists. Indeed, what was considered as *the* elastic problem for a hundred of years has been regarded with condescension by later historians. Mostly because it is wrongly

* Corresponding author at: Laboratory of Agent Based Social Simulation, Institute of Cognitive Science and Technology, CNR, via Palestro 32, Roma, 00185, Italy.

E-mail addresses: daniele.vilone@gmail.com, daniele.vilone@istc.cnr.it (D. Vilone).

https://doi.org/10.1016/j.ijengsci.2023.103941
Received 26 May 2023; Received in revised form 25 July 2023; Accepted 9 August 2023
Available online 1 September 2023
0020-7225/

assumed that later works on three-dimensional elasticity somehow fixed it. However, in modern theories of bending, such as Saint Venant's, the existence of the neutral line is implicitly postulated *ad hoc*, not proved (Euler, 1960; Truesdell, 1984). In this paper, our purpose is to tackle a problem of a more limited reach: assuming Hooke's law, we wish to establish a criterion for the existence and placement of a neutral curve starting from a generic, non-straight, configuration of the elastica, contrary to the usual theory of slender beams.

The problem of spontaneously curved bands was already known to Jacob Bernoulli, as testified by a posthumous fragment published in 1744 (Truesdell, 1984). In the same year, Euler's treatise on elastic curves also appeared: there, the law of an elastica endowed with an initial non-zero curvature was asserted (Euler, 1960). A systematic theory of rods with curved undeformed configuration is substantially due to Clebsch (1862), although already outlined by Kirchhoff (1859), to whom the notion of "unstressed state" must probably be acknowledged. Only in Timoshenko's theory of curved beams (Timoshenko, 1955), however, it is shown that the neutral fiber does not correspond to the line of centroids. Surprisingly, in the 20th century the problem of the elastica whose undeformed shapes are circular arcs or rings, in particular, has been taken up by several authors (Antman, 1968; Atanackovic, 1998; Chaskalovic & Naili, 1995; Fu & Waas, 1995; Kämmel, 1967; Katifori, Alben, & Nelson, 2009; Kosel, 1984; Lagrange, Jiménez, Terwagne, Brojan, & Reis, 2016; Schmidt, 1996; Schmidt et al., 1979; Troger & Steindl, 2012; Vakakis & Atanackovic, 1999), seemingly neglecting Timoshenko's work. As a matter of fact, when the one-dimensional representation of a naturally skewed elastica is provided, usually this corresponds to the line of centroids (Antman, 1968; Atanackovic, 1998); this is assumed, sometimes tacitly, to be the neutral fiber, which can be extensible Antman (1968), Atanackovic (1998), Kämmel (1967), Lagrange et al. (2016), Magnusson, Ristinmaa, and Ljung (2001), Oshri and Diamant (2016), Tadjbakhsh (1966), or inextensible Chaskalovic and Naili (1995), Fu and Waas (1995), Katifori et al. (2009), Kosel (1984), Schmidt (1996), Schmidt et al. (1979), Troger and Steindl (2012), Vakakis and Atanackovic (1999).

In this paper we consider the deformation of an elastica with a spontaneous non-uniform curvature, thus generalizing the theory of curved beams. Our work is motivated by the fact that natural biological filaments cannot be considered straight in their native state, nor endowed with a uniform curvature. To the contrary, biological materials develop into a variety of complex shapes, which can sense and respond to local curvature. This field of mechanobiology (Schoen, Pruitt, & Vogel, 2013) poses fundamental questions about the function of geometry, especially on the role that the local curvature plays in biological systems (Schamberger et al., 2022). In particular, the curvature appears as a determining factor in important biological functional tasks executed by many bio-polymers inside the cell (Bausch & Kroy, 2006; Brangwynne, Koenderink, MacKintosh, & Weitz, 2008; Ghosh & Gov, 2014; Harada, Noguchi, Kishino, & Yanagida, 1987; Schaller et al., 2010), as well as in the design of next-generation genomics technologies (Dorfman, 2018).

On top of that, none of the three major classes of cytoskeletal filaments, microtubules, actin filaments, and intermediate filaments, can be considered homogeneous nor isotropic, as each is formed from chains of discrete protein monomers (Alberts, 2017). At the typical level of description in usual molecular mechanics models, however, they are often treated as traditional engineering elements (Howard & Clark, 2002): they are considered plane elastica, the mechanical behavior of which is entirely dictated by Bernoulli–Euler's theory. Our model does not deviate from this conceptual framework; however, our construction can be easily generalized to realistically account for non-homogeneous filaments with varying geometrical and mechanical properties.

Our starting point is the derivation of the strain energy associated to any three-dimensional elastica deformation, as the energy cost of a shape fluctuation is the significant starting concept of any dynamical model in polymer physics (Doi, Edwards, & Edwards, 1988; Rubinstein et al., 2003). The one-dimensional representation of the elastica arises as the natural context for the strain energy formulation (Section 2). The macroscopic constitutive relations are obtained from the strain energy function (Section 3), and in Section 4 we demonstrate that the strain energy minimization with respect to a suitable choice of a reference frame furnishes the criterion for locating the neutral curve. We conclude the paper in Section 5, discussing the implication of our findings in terms of polymer dynamics and statistics, providing the evidence that the developed framework yields the correct generalization of flexible and semiflexible polymers models, and of simplified one-dimensional models of fluctuating vesicles. We discuss the relevance that the old-fashioned concept of neutral fiber acquires in modern polymer physics. We show, indeed, that a renovated interest around it is motivated by the fact that its existence is provided by the minimum energy principle at the base of any polymer conformational change. We discuss the correct and convenient way of implementing our model in computer simulations and, finally, the relevance of our model in describing real biological non-homogeneous filaments.

2. The model

We consider the deformation of an homogeneous *plane extensible elastica* (Antman, 1968), i.e., a prismatic hyperelastic three-dimensional body with rectangular sections having 'thin' sides (height h and depth b) and generic length, subject to the only restriction that its deformations take place in a plane, thus excluding twisting. According to the Cosserat's theories (Cosserat & Cosserat, 1909; Green, Naghdi, & Wenner, 1974a, 1974b; Naghdi & Rubin, 1984; Rubin, 2000), any elastic deformation stems from a natural body configuration or state, defined as the shape corresponding to the unstressed condition (Love, 2013). The work performed in passing from the natural to the deformed state is the strain or stored energy, which is the pivotal concept in our model.

We propose to compute the strain energy using a finite difference scheme, as displayed in Fig. 1. The undeformed body is schematically subdivided in N elementary blocks of arbitrary volumes $\Delta V^{(i)}$ ($i = [1, N]$) (Fig. 1A). To each elementary volume a local reference system is assigned, where the ξ and η_α axes define the block's longitudinal and transverse directions, respectively, and the origin is arbitrarily placed at an height αh ($0 \le \alpha \le 1$) from the block's bottom surface, see Fig. 1A, and at the left side of the block as shown in figure. We now introduce a reference segment of length $\Delta L_\alpha^{(i)}$, equivalent to the longitudinal dimension of the plane $\eta_\alpha = 0$ (Fig. 1A). Assuming the cross-sections to remain rigid, the body deformation necessarily involves the deformation of

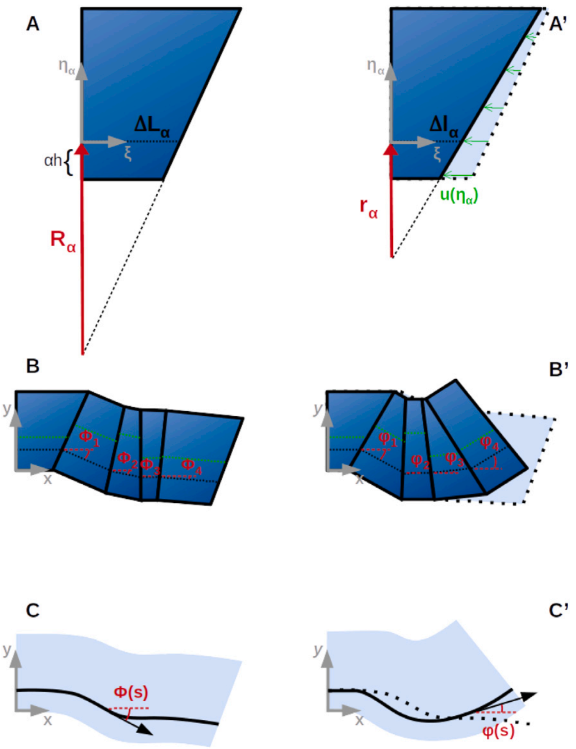

Fig. 1. Derivation of the strain energy. **A:** The elementary block with its local reference frame ξ-0-η_α, having the origin placed at an height αh from the bottom surface ($\alpha \in [0,1]$). A reference fiber ($\eta_\alpha = 0$) is characterized by its length ΔL_α (dotted black line) and by R_α, with the corresponding spontaneous curvature $K_\alpha = \frac{1}{|R_\alpha|}$. R_α is the distance of the origin of the local reference frame from the intersection between the extended sides of the block, with a positive sign if its orientation is concordant with that of η_α; it becomes the curvature radius in the continuum limit. **A′**: The block undergoes a deformation to a new shape (dark blue), while the original configuration is in light blue. Shape change entails $R_\alpha \to r_\alpha$. Any fiber of the block endures a deformation represented by the fiber displacement $u(\eta_\alpha) = \Delta l(\eta_\alpha) - \Delta L(\eta_\alpha)$ (green arrows). **B:** The undeformed elastica is displayed as a sequence of elementary blocks, each with its own shape. The sequence of the reference segments is shown as a dotted black polygonal L_α, while the orientation, or cross-sectional bending angle $\Phi^{(i)}$ of each block is in red. The green dashed lines correspond to the $\alpha_U^{(i)}$ fibers. Conventionally, the construction assumes that the left section of each block remains straight-angled, so that the orientation angles are defined at the left side of each block. **B′**: The deformation of the elastica involves the deformation of the reference polygonal chain, $L_\alpha \to l_\alpha$ (dotted black line). The orientation varies from $\Phi^{(i)}$ to $\varphi^{(i)}$. **C:** In the continuum limit, the material reference curve is represented by a solid black curve. The tangent to this curve, $\mathbf{T}_\alpha(s)$, forms with the x-axis the spontaneous bending angle $\Phi(s)$. **C′**: The deformed material curve (solid black line) stems from its undeformed configuration (dotted black line). The black arrow represents the new tangent $\mathbf{t}_\alpha(s)$, while its corresponding bending angle $\varphi(s)$ is in red.

each block, passing from the volume $\Delta V^{(i)}$ to $\Delta v^{(i)}$. At the same time, the reference segment $\Delta L_\alpha^{(i)}$ transforms into $\Delta l_\alpha^{(i)}$. As in usual theories of elastic flexure, we assume that the stress is determined by the strain Truesdell and Noll (2004), and the strain consists of the displacements of independent longitudinal filaments $u^{(i)}(\eta_\alpha) = \Delta l^{(i)}(\eta_\alpha) - \Delta L^{(i)}(\eta_\alpha)$. Embracing the microscopical validity of Hooke's law, we sum, *à la* Leibniz, over the contributions of the fibers upon the entire cross section. Thus, the elementary block's strain energy can be written as

$$\Delta E_\alpha^{(i)} = \frac{bY}{2}\int_{-\alpha h}^{(1-\alpha)h}\left[\frac{u^{(i)}(\eta_\alpha)}{\Delta L^{(i)}(\eta_\alpha)}\right]^2 \Delta L^{(i)}(\eta_\alpha)\, d\eta_\alpha, \tag{1}$$

where Y is a parameter which has the dimensions of a stress and depends on the material properties. Therefore the strain energy (1) represents the work performed in deforming the elementary block from the unstressed configuration reported in Fig. 1A, to that in Fig. 1A′. However, in continuity with usual theories, the strain energy (1) is associated to the deformation of the representative material segment. Nevertheless, $\Delta E_\alpha^{(i)}$ is a scalar quantity and, as such, must be invariant under a change of the local reference frame, i.e., a change of the material representative segment. As a matter of fact, by applying the transformation $\eta_\alpha = \eta_\beta - (\alpha - \beta)h$, the property $\Delta E_\alpha^{(i)} = \Delta E_\beta^{(i)}$ is always satisfied, as it is demonstrated in the Supplementary Informations (SI). The analytical derivation of the energy (1) is fully developed in SI. We hereby report the final expression:

$$\Delta E_\alpha^{(i)} = \frac{Y}{2}\Delta L_\alpha^{(i)}\left\{F_\alpha^{(i)}\,{\varepsilon_\alpha^{(i)}}^2 + 2S_\alpha^{(i)}\,\varepsilon_\alpha^{(i)}\mu_\alpha^{(i)} + I_\alpha^{(i)}\,{\mu_\alpha^{(i)}}^2\right\}, \tag{2}$$

where we have introduced the axial strain

$$\varepsilon_\alpha^{(i)} = \frac{\Delta l_\alpha^{(i)} - \Delta L_\alpha^{(i)}}{\Delta L_\alpha^{(i)}} \tag{3}$$

and the bending measure (Antman, 1968)

$$\mu_\alpha^{(i)} = \frac{1}{\Delta L_\alpha^{(i)}}\left(\frac{\Delta l_\alpha^{(i)}}{r_\alpha^{(i)}} - \frac{\Delta L_\alpha^{(i)}}{R_\alpha^{(i)}}\right). \tag{4}$$

The quantities $R_\alpha^{(i)}$ and $r_\alpha^{(i)}$ are the radii connecting the intersection point between the extensions of the block limiting sections, with the origin of the block's local reference system: they have a sign corresponding to their orientation, as shown in the SI (see Fig. 1A,A′ for the details). In the following we will show how, in the continuum limit, they correspond to the local radii of curvature of the undeformed and deformed configurations, respectively. For simplicity, from now on we will refer to such quantities as curvature radii also in the discrete case. Likewise, we will define the block spontaneous curvature as $K_\alpha^{(i)} = \frac{1}{\left|R_\alpha^{(i)}\right|}$, while $k_\alpha^{(i)} = \frac{1}{\left|r_\alpha^{(i)}\right|}$.

Most importantly, according to Timoshenko's curved beam theory (Timoshenko, 1955), $F_\alpha^{(i)}$ represents the reduced area, $I_\alpha^{(i)}$ the reduced moment of inertia and $S_\alpha^{(i)}$ the reduced axial-bending coupling moment. They have a simple integral expression furnished in SI, corresponding to the formula obtained by Kämmel in the theory of a ring allowing axial compressibility and subjected to hydrostatic pressure (Kämmel, 1967), and subsequently used in the analysis of compressible rings (Atanackovic, 1998). Our derivation, however, sheds light on a fundamental aspect that remained seemingly unnoticed in the past analysis: that is, $F_\alpha^{(i)}$, $S_\alpha^{(i)}$ and $I_\alpha^{(i)}$ take different forms according to whether the intersection between the sidelines containing the block's sections lies above or below the elementary volume, i.e., they depend on the direction of $R_\alpha^{(i)}$ (see SI). This dependence is compactly expressed as

$$F_\alpha^{(i)} = \frac{b}{K_\alpha^{(i)}} \ln\left(1 + h\, \max[K_0^{(i)}, K_1^{(i)}]\right), \tag{5}$$

$$S_\alpha^{(i)} = \frac{\operatorname{sgn}\left(K_0^{(i)} - K_1^{(i)}\right)}{K_\alpha^{(i)}} \left[bh - F_\alpha^{(i)}\right], \tag{6}$$

$$I_\alpha^{(i)} = \frac{\operatorname{sgn}\left(K_0^{(i)} - K_1^{(i)}\right)}{K_\alpha^{(i)}} \left[b\left(\frac{1}{2} - \alpha\right) h^2 - S_\alpha^{(i)}\right]. \tag{7}$$

If the center of the intersection point is placed below the block's bottom line ($\alpha = 0$), hence $K_0^{(i)} > K_1^{(i)}$ and the function $\operatorname{sgn}\left(K_0^{(i)} - K_1^{(i)}\right) = 1$. In the opposite case, the curvature of the upper fiber $\alpha = 1$ is such that $K_1^{(i)} > K_0^{(i)}$, and $\operatorname{sgn}\left(K_0^{(i)} - K_1^{(i)}\right) = -1$. By inspection of the expression (6), there exists one value of α for which stretching and bending term are decoupled, i.e. $S_\alpha^{(i)} = 0$. This value corresponds to

$$\alpha_U = \begin{cases} \frac{1}{\ln(1+h\,K_0)} - \frac{1}{hK_0} & K_0 > K_1 \\ 1 - \left[\frac{1}{\ln(1+h\,K_1)} - \frac{1}{hK_1}\right] & K_1 > K_0\,, \end{cases} \tag{8}$$

with $S_\alpha > 0$ for $\alpha < \alpha_U$, and $S_\alpha < 0$ for $\alpha > \alpha_U$. Moreover, it is worth to notice that it results

$$\lim_{K_{0/1}\to 0^+} \alpha_U = \frac{1}{2}.$$

This means that the fiber allowing the axial-bending uncoupling coincides with the line of centroids in the case of flat undeformed configuration, recovering the classical beam theories result, as shown in the SI.

Formally, the full body strain energy is the sum of the elementary blocks strain energy, i.e. $E_\alpha = \sum_{i=1}^N \Delta E_\alpha^{(i)}$. In our finite difference scheme, the ordered sequence of consecutive $\Delta L_\alpha^{(i)}$ constitutes the representative undeformed material polygonal chain L_α in Fig. 1B. Correspondingly, the ordered sequence of consecutive $\Delta l_\alpha^{(i)}$ composes the representative deformed material polygonal chain l_α in Fig. 1B′. Now, adopting as unique reference system the laboratory frame as in Fig. 1B,B′, the strain energy E_α is expressible in terms of the axial strain (3), and of the bending measure $\mu_\alpha^{(i)}$, which assumes an alternative but equivalent expression to that in (4) (Antman, 1968; Atanackovic, 1998; Greenberg, 1967; Kämmel, 1967):

$$\mu_\alpha^{(i)} = \frac{\Delta\Phi^{(i)} - \Delta\varphi^{(i)}}{\Delta L_\alpha^{(i)}}, \tag{9}$$

where $\Phi^{(i)}$ ($\varphi^{(i)}$) is the (i)-th cross-sectional orientation angle with respect the x–axis in the undeformed (deformed) configuration (see Fig. 1B and 1B′). Hence

$$E_\alpha = \frac{Y}{2}\sum_{i=1}^N \Delta L_\alpha^{(i)} \left\{ F_\alpha^{(i)}\, {\varepsilon_\alpha^{(i)}}^2 + 2S_\alpha^{(i)}\, \varepsilon_\alpha^{(i)} \mu_\alpha^{(i)} + I_\alpha^{(i)}\, {\mu_\alpha^{(i)}}^2 \right\}\ . \tag{10}$$

In our finite difference scheme, the blocks are assumed to be independent. Thus, nothing prevents us from assigning to each block a different local reference frame, i.e., a different α. As a matter of fact, thanks to the property of invariance of $\Delta E_\alpha^{(i)}$ under a change of local reference frame, the total energy E_α is also invariant. We will revisit this important consideration in Section 4 when we discuss the existence of the neutral curve.

The continuum limit is taken by increasing N up to the point that the poligonal chain L_α (l_α) tends to a finite curve, namely the reference curve, or representative fiber $\mathscr{L}_\alpha$ (ℓ_α) (Fig. 1C, 1C′). According to the older theories of flexure, a material fiber can be envisaged as a translation of one of the outermost curves ($\alpha = 0$ or $\alpha = 1$) along the orthogonal cross sections of the body. The Cartesian components of the material line, or fiber, in the laboratory frame are expressed as $\mathbf{L}_{\boldsymbol{\alpha}}(s)\left(X_\alpha(s), Y_\alpha(s)\right)$ and $\mathbf{l}_{\boldsymbol{\alpha}}(s)\left(x_\alpha(s), y_\alpha(s)\right)$, respectively, where s is the same internal parameter for both the undeformed reference fiber $\mathscr{L}_\alpha : [s_m, s_M] \to \mathbb{R}^2$ and deformed one $\ell_\alpha : [s_m, s_M] \to \mathbb{R}^2$. By introducing the tangents $\mathbf{T}_{\boldsymbol{\alpha}} = \frac{d\mathbf{L}_{\boldsymbol{\alpha}}}{ds}$ and $\mathbf{t}_{\boldsymbol{\alpha}} = \frac{d\mathbf{l}_{\boldsymbol{\alpha}}}{ds}$ to $\mathscr{L}_\alpha$ and ℓ_α, the continuum limit of the elastica strain energy is

$$\mathscr{E}_\alpha = \frac{Y}{2}\int_{s_m}^{s_M} ds \left\{ \frac{F_\alpha(s)}{\left|\mathbf{T}_{\boldsymbol{\alpha}}(s)\right|} \left[\left|\mathbf{t}_{\boldsymbol{\alpha}}(s)\right| - \left|\mathbf{T}_{\boldsymbol{\alpha}}(s)\right|\right]^2 + \right.$$

$$\left. -\frac{2S_\alpha(s)}{\left|\mathbf{T}_{\boldsymbol{\alpha}}(s)\right|} \left[\left|\mathbf{t}_{\boldsymbol{\alpha}}(s)\right| - \left|\mathbf{T}_{\boldsymbol{\alpha}}(s)\right|\right] \left[\varphi'(s) - \Phi'(s)\right] + \frac{I_\alpha(s)}{\left|\mathbf{T}_{\boldsymbol{\alpha}}(s)\right|} \left[\varphi'(s) - \Phi'(s)\right]^2 \right\}, \tag{11}$$

where $(\cdot)'$ denotes the derivative with respect to s. The expression (11) constitutes one of the main results of our analysis, extending Timoshenko's linear theory of curved beams to the case of an elastica with generic undeformed condition, identified by varying local spontaneous curvature $K(s) = \left|\Phi'(s)\right|$. In the SI the differential form of the quantities in (5), (6) and (7) are furnished. In particular, it is worth noticing how the condition for the axial-bending uncoupling (8) must be valid locally in the continuum limit, i.e. $S_\alpha(s) = 0$. This can be achieved only if α_U in (8) changes with s according to

$$\alpha_U(s) = \frac{\left|\mathbf{T}_0(s)\right|}{h\Phi'(s)} - \frac{\left|\Phi'(s)\right|}{\Phi'(s)} \frac{1}{\ln\left(1 + h\frac{\left|\Phi'(s)\right|}{\min[\left|\mathbf{T}_0(s)\right|,\left|\mathbf{T}_1(s)\right|]}\right)}. \tag{12}$$

The classical case of a thin slender rod, beam or bar (Euler, 1960), is also derived in the SI for the sake of completeness. It is shown how this constitutes the zero curvature limit of the general model represented by the energy expression (11).

3. Macroscopic constitutive relations

We now derive the macroscopic stress–strain relations for the elastica, given a generic undeformed configuration. Our starting point is the strain energy density, defined as $W_\alpha = \frac{\Delta E_\alpha}{\Delta L_\alpha}$. Therefore, when the undeformed state has a constant curvature throughout the whole elastica, from Eq. (2) it turns out that for a generic choice of the representative fiber

$$W_\alpha = \frac{Y}{2}\left\{F_\alpha\,{\varepsilon_\alpha}^2 + 2S_\alpha\,\varepsilon_\alpha\mu_\alpha + I_\alpha\,{\mu_\alpha}^2\right\}. \tag{13}$$

The macroscopic constitutive equations can be drawn from (13), according to the derivation furnished in Antman (1968), which employs the definition of the elastica as a three-dimensional body, or to an alternative variational approach in which the elastica is treated as a one-dimensional medium (Tadjbakhsh, 1966):

$$\begin{cases} N_\alpha = \frac{\partial W_\alpha}{\partial \varepsilon_\alpha} = Y\left(F_\alpha\varepsilon_\alpha + S_\alpha\mu_\alpha\right) \\ M_\alpha = \frac{\partial W_\alpha}{\partial \mu_\alpha} = Y\left(S_\alpha\varepsilon_\alpha + I_\alpha\mu_\alpha\right). \end{cases} \tag{14}$$

N_α and M_α are the elastica axial force and bending moment respectively, where the one-dimensional representation of the elastica coincides with a generic fiber α. We recall that the bending measure enjoys two analogue definitions, Eqs. (4) and (9). From Eqs.(14), it is immediately verified that linear decoupled relations only hold for the choice of the material fiber allowing for the axial-bending uncoupling of the strain energy (2), namely $\alpha = \alpha_U$ in Eq. (8). The same condition is valid in the classical case of flat initial configuration, as it is shown in SI.

It is instructive to see how the constitutive relations transform under change of reference line, i.e. when shifting from the fiber α to β. To this end, we firstly need to express how the strain and the bending measure are modified if the material line changes:

$$\varepsilon_\alpha = \frac{\Delta L_\beta}{\Delta L_\alpha}\left[\varepsilon_\beta + h(\alpha - \beta)\mu_\beta\right], \tag{15}$$

and

$$\mu_\alpha = \frac{\Delta L_\beta}{\Delta L_\alpha}\mu_\beta. \tag{16}$$

Therefore, plugging these relations into (14), it turns out that

$$\begin{cases} N_\alpha = N_\beta \\ M_\alpha = M_\beta + h(\beta - \alpha)N_\beta. \end{cases} \tag{17}$$

The former transformations appear to be universal, in the sense that they are valid in the case of slender bars as well, as shown in SI. Importantly, while the axial force is invariant under change of representative fiber, the bending moment gains an axial force contribution which accounts for the different curvatures of the fibers α and β. Moreover, when $N_\alpha = 0$, the bending moment is invariant under changes of representative fiber: $M_\alpha = M_\beta$. Physically this corresponds to the fact that, for a pure bending transformation, the bending moment cannot depend on the fiber chosen as representative. For any other transformation for which $N_\alpha \neq 0$, the bending moment will depend on the fiber on which it is computed, and the axial force contribution has to be summed up to the total moment of the forces.

When the curvature is locally changing within the elastica, the continuum version of the strain energy density (13) is

$$\begin{aligned}\mathscr{W}_\alpha(s) = & \frac{Y}{2\left|\mathbf{T}_\alpha(s)\right|^2}\left\{F_\alpha(s)\,\left[\left|\mathbf{t}_\alpha(s)\right| - \left|\mathbf{T}_\alpha(s)\right|\right]^2 + \right.\\ & \left. -\,2S_\alpha(s)\,\left[\left|\mathbf{t}_\alpha(s)\right| - \left|\mathbf{T}_\alpha(s)\right|\right]\left[\varphi'(s) - \Phi'(s)\right] + I_\alpha(s)\,\left[\varphi'(s) - \Phi'(s)\right]^2\right\},\end{aligned} \tag{18}$$

from which the constitutive equations in a local form can be defined as

$$\begin{cases} N_\alpha(s) = \frac{\partial \mathscr{W}_\alpha(s)}{\partial\left|\mathbf{t}_\alpha(s)\right|} = \frac{Y}{\left|\mathbf{T}_\alpha(s)\right|^2}\left\{F_\alpha(s)\left[\left|\mathbf{t}_\alpha(s)\right| - \left|\mathbf{T}_\alpha(s)\right|\right] - S_\alpha(s)\left[\varphi'(s) - \Phi'(s)\right]\right\} \\ M_\alpha(s) = \frac{\partial \mathscr{W}_\alpha(s)}{\partial \varphi'(s)} = \frac{Y}{\left|\mathbf{T}_\alpha(s)\right|^2}\left\{-S_\alpha(s)\left[\left|\mathbf{t}_\alpha(s)\right| - \left|\mathbf{T}_\alpha(s)\right|\right] + I_\alpha(s)\left[\varphi'(s) - \Phi'(s)\right]\right\}. \end{cases} \tag{19}$$

Once again, the value of α needs to be varied throughout the elastica according to the law (12), for the stress–strain relationships (19) to be locally decoupled.

4. Neutral fiber location

The neutral fiber is the locus of points which does not undergo any longitudinal extension nor contraction during the elastica deformation (Love, 2013). If there is one, this does not necessarily coincide with the line of centroids (Love, 2013) and its existence depends entirely on the transformation put in use.

After Jacob Bernoulli's first erroneous attempt of establishing a general principle for the neutral fiber placement, based on the balance of bending moments between elongated and compressed fibers, the correct condition was enunciated by Parent in 1713 (Parent, 1713) and rediscovered by Coulomb 60 years later (Coulomb, 1773): *the neutral fiber is the locus of points separating the region of extension from that of compression, such that the longitudinal forces are balanced*. This criterion, however, is easy to implement in case of Hookean dependence of the tension over the cross-section, but is hard to be assessed for a generic (non-linear) stress–strain relation, as precisely sought by Jacob Bernoulli.

Let us see how Parent's principle applies to the case under investigation. We start by considering an elastica with uniform spontaneous curvature, a situation encompassing the cases of a slender bar, a circular arc or an hyperbola. The requirement of the longitudinal forces balance corresponds to $N_\alpha = 0$. However, this constitutes just the necessary condition for the existence of the neutral line. As a matter of fact, it does not furnish a precise answer about its placement because, in view of the first of Eq. (17), it does not depend on the specific choice of the representative fiber. However, among all the representative fibers, for rigid cross sections, only one satisfies the zero strain condition $\varepsilon_\alpha = 0$, i.e., the value of α_U in (8). Therefore, as a general principle, we can conclude that the neutral fiber, when it exists, corresponds to the representative line which ensures the axial-bending uncoupling of the strain energy. This is an universal property, valid for both flat and non-flat initial configurations. Moreover, it appears that for any transformation guaranteeing the existence of the neutral fiber, the bending moment is independent of the representative fiber choice, as implied by Eqs. (17).

We now investigate how the neutral fiber is identified when the curvature is not uniform throughout the elastica in the undeformed configuration. This is achieved by using the macroscopic constitutive relations in the local formulation (19). The condition implied by Parent's principle requires $N_\alpha(s) = 0\ \forall s$, accompanied by the zero strain condition $\left|\mathbf{t}_\alpha(s)\right| = \left|\mathbf{T}_\alpha(s)\right|$. While in the case of elastica endowed with uniform spontaneous curvature the neutral fiber is identified with a material line, or fiber, corresponding to a constant α, the situation is totally different for a generic undeformed configuration. As a matter of fact, in this case one cannot properly talk about neutral fiber, in the sense that the curve guaranteeing $N_\alpha(s) = 0$ together with the zero local strain conditions, does not overlap with one of the elastica material fibers. Rather, the concept of neutral fiber is replaced by that of neutral curve, defined as the locus of points identified by the value of $\alpha_U(s)$ in Eq. (12). A typical situation is that depicted in Fig. 2C, where the initial curvature is a function of the internal parameter s, $K_\alpha(s)$, and the neutral curve is shown as a black dotted line, jiggling around the line of centroids (dashed red line), and approaching the side of the elastica with maximum value of the natural curvature. Notably, while any representative fiber is always orthogonal to the cross-section, the neutral curve is not, in general.

Therefore, if the elastica transformation provides the existence of a neutral curve, it is possible to adopt a *neutral* arc-length parametrization such that $\left|\mathbf{T}_{\alpha_U}(s)\right| = 1$. Adopting this parametrization, the energy assumes the following simple form (see SI)

$$\mathscr{E}_{\alpha_U} = -\frac{bYh^2}{2}\int_{s_m}^{s_M} ds\left[\frac{1}{2} - \alpha_U(s)\right]\frac{\left[\varphi'(s) - \Phi'(s)\right]^2}{\Phi'(s)}. \tag{20}$$

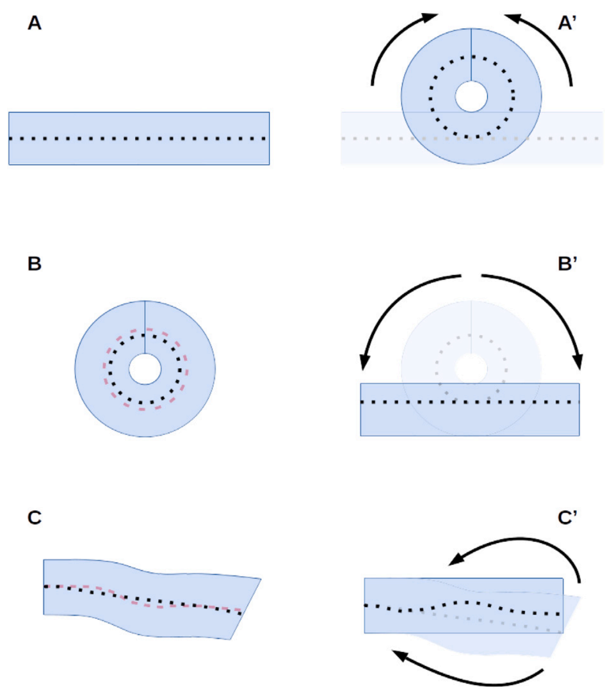

Fig. 2. Neutral fiber location. **A:** The undeformed condition coincides with a straight bar of length L. The line of centroids ($\alpha = 1/2$) is depicted as a dotted black fiber: taking this as the representative one-dimensional medium would give the axial-bending uncoupling (see SI). **A′**: The beam in panel A is bent into a ring. If the line of centroids retains its length, it coincides with the neutral fiber and the axial forces are balanced ($N_\alpha = 0, \forall\alpha$). Among all possible deformations which transform a beam into a circle, the one allowing the existence of the neutral line costs the minimum amount of work. **B:** The undeformed condition is a circle. The line of centroids ($\alpha = 1/2$) is depicted as a dashed red circle, while the material fiber granting the axial-bending uncoupling, defined by α_U in Eq. (8), is shown as a dotted black line. **B′**: The circle in panel B is deformed into a straight beam. If the line identified by α_U keeps its length constant during the circle extension, it coincides with the neutral fiber and Parent's principle is satisfied. Any other stretching of the circle into a bar will cost more energy than that leaving unchanged the neutral line. Notice that, although the circles in panels A′ and B have the same dimensions, the absence of axial forces implies that the beam in A is longer than that in B′ (see SI). **C:** The generic undeformed configuration has a line of centroids shown as dashed red. The curve allowing the axial-bending uncoupling in the Eq. (11) is show as black dotted. This curve does not overlap with any material fiber according to (12) **C′**: Any transformation where the length of the black dotted line is left invariant fulfills Parent's principle. Hence, the notion of neutral fiber shifts to that of *neutral curve*. Here the final deformed condition is flat, showing how the neutral curve is deformed differently from any other material fiber.

At the same time, the bending moment takes the form

$$M_{\alpha_U}(s) = -bYh^2\left[\frac{1}{2} - \alpha_U(s)\right]\frac{\left[\varphi'(s) - \Phi'(s)\right]}{\Phi'(s)}. \tag{21}$$

Let us take a moment to clarify what is implicit in the expression (20). The neutral curve requires that the value of α changes with s according to Eq. (12). As a consequence, the neutral arc-length parametrization entails that the strain energy (20) interpolates the expressions (11), in the same fashion as $\alpha_U(s)$ interpolates among the different α. However, for a deformation that preserves the neutral curve, the value of $\mathscr{E}_{\alpha_U} \equiv \mathscr{E}_\alpha$, thanks to the property of invariance of ΔE_α under a change of reference frame, which holds locally also in the continuum limit.

5. Discussion

Our one-dimensional treatment of a three-dimensional elastica is in the wake of the old theories of flexure and bending. Nevertheless, the choice of a fiber α as the representative one-dimensional medium is purely arbitrary. As a matter of fact, the linchpin of our analysis has been to disentangle the representative material fiber from the notion of neutral curve, which in general does not overalp with a material fiber. Indeed, contrary to the modern three-dimensional theories of bending, we do not postulate the existence of a neutral fiber, or a neutral curve, neither we identify it with the line passing through the centroids. Our main achievement has been to furnish the exact criteria for its existence and its location. These criteria ultimately stem from the derivation of the strain energy, and are encapsulated in the following universal condition:

$$\left.\frac{\partial \Delta E_\alpha}{\partial \varepsilon_\alpha}\right|_{\varepsilon_\alpha = 0} = 0. \tag{22}$$

Locating the position of the neutral line, being a fiber or a curve, does not have only an effect on the stiffness of a given cross-sectional form: Eq. (22) implies that it becomes a crucial issue for any physical transformation aiming at minimizing the amount of work required, given a shape transformation. Let us explain this point with the help of Fig. 2: imagine to have a slender bar, such that in panel A, transformed into the circle in panel A′. Among all the possible deformations that bend the elastic bar into a ring, only one allows the presence of the neutral fiber, and is that leaving unvaried the line of the centroids. In this case, Parent's principle is satisfied and the longitudinal forces are balanced, i.e. $N_\alpha = 0\ \forall \alpha$. We could imagine to give the bar a final circular shape preserving the length of a different fiber, say the bottom material line ($\alpha = 0$), together with Jacob Bernoulli (in his first attempt, dating 1694) or Euler Euler (1960). In this case, however, $N_\alpha \neq 0$, and the bottom line cannot be identified with the neutral fiber although $\varepsilon_{\alpha=0} = 0$. The important point is that the amount of work spent by deforming the beam into a circle is minimum if the line of centroids keeps its length unvaried. This is plainly demonstrated in the SI. Now, it is also instructive to consider the opposite case, where the circular shape is the unstressed condition (Fig. 2B), and the flat configuration is the deformed one (Fig. 2B′). The neutral line in this case does not correspond to that of the centroids (red dashed line) but it is a circumference with smaller radius, according to the value of (8) (black dotted line). Thus, the minimum amount of work required to "stretch" the circle into a bar is obtained if the corresponding transformation leaves the neutral fiber unvaried. As a corollary, the bar shown in panel B′ of Fig. 2 is smaller than that in panel A, because the length of the extended beam in panel B′ is $l = \frac{2\pi h}{\ln\left(\frac{L+\pi h}{L-\pi h}\right)} < L$.

So far we addressed the cases of elastica endowed with spontaneous constant curvature. We now turn to the elastica with intrinsic local curvature as in Fig. 2C. The variational version of the minimum principle in (22) is

$$\left.\frac{\delta \mathscr{E}_\alpha}{\delta \left|\mathbf{t}_\alpha(s)\right|}\right|_{\left|\mathbf{t}_\alpha(s)\right|=\left|\mathbf{T}_\alpha(s)\right|} = 0. \tag{23}$$

Imagine an elastic filament undergoing a shape transformation. One is generally inclined to think that such a system would prefer to deform by minimizing its energy, skewing and swelling in the fashion that is the easiest of all. The expression (23) specifies that such a minimum-cost deformation is only obtainable by preserving the length of the neutral curve. However, due to the immaterial nature of the neutral curve, its profile may differ considerably from the actual three-dimensional configuration. This is graphically represented in Fig. 2C′ where, for the sake of simplicity, the elastica deformed configuration is set to be straight and the neutral curve is quite something else.

5.1. *The importance of the neutral curve for ideal chains*

The above considerations have a tremendous impact into both non-equilibrium properties and equilibrium statistics of polymers or other macromolecules. Take for example the conformational dynamics of ideal chains (Doi et al., 1988; Rubinstein et al., 2003). Ideal chains provide simplified one-dimensional models for real flexible and semiflexible biomolecules, being substantially the trace of their backbone, with negligible self-interactions or excluded volume effects. Among semiflexible models, certainly the most successful is the Worm-Like Chain (WLC) introduced by Kratky and Porod (Kratky & Porod, 1949; Marko & Siggia, 1995) for inextensible stiff-rod polymers, for which the energy associated with conformational fluctuations may be captured by using merely linear elasticity. The effective WLC energy associated with the bending is (Fixman & Kovac, 1973; Marko & Siggia, 1995; Yamakawa, 1977)

$$\mathscr{E}_{WLC} = \frac{k_B T}{2}\int_0^L ds\, A\, k(s)^2 \tag{24}$$

where k_B is the Boltzman constant, T is the temperature and A is the persistent length, characterizing the bending stiffness of the polymer. As the expression (24) is derived from thin-rod linear elasticity, it entirely fits into the framework developed in this paper. Indeed the stretching energy of a straight ribbon with inextensible neutral fiber, i.e., the line of centroids, can be expressed as

$$\mathscr{E}_{1/2} = \frac{bYh^3}{2}\int_0^L ds\, \frac{\varphi'(s)^2}{12} \tag{25}$$

if the same line of centroids ($\alpha = 1/2$) is assumed as the representative fiber (see SI). The analogy between the expression (24) and (25) is apparent if one recalls that (i) both expressions are derived assuming the arc-length parametrization for which $\left|\mathbf{t}_{(1/2)}(s)\right| = 1$, (ii) the local curvature $k(s) \equiv \left|\varphi'(s)\right|$, and (iii) Young's modulus Y exhibits a temperature dependence (Varshni, 1970) (in this respect notice that also A may depend on T (Geggier, Kotlyar, & Vologodskii, 2011; Martin et al., 2018)). At the same time, from the comparison of Eqs. (24) and (25) it emerges that the natural configuration of a polymer is tacitly assumed to be a rigid rod (Fuller, 1971; Tanaka & Takahashi, 1985), not only at $T = 0$. This contrasts with real polymeric chains, whose microstructural shape is naturally coiled. Taking into account the polymers natural curvature requires the formal extension of the ideal energy (24) along the line marked by our theoretical analysis. In particular, in view of Eq. (23), the inextensibility requirement attains the higher value of a principle of minimum energy. To be inextensible, however, is none of the polymer material lines, but the neutral curve. This practically translates into fluctuations of the three dimensional polymer conformation and of its contour length, although limited, in contrast with the classical WLC picture. Importantly, it elucidates the contour molecule fluctuations observed in short to moderate length molecules, where $L/A \sim 6 - 20$ (Seol, Li, Nelson, Perkins, & Betterton, 2007), and it may help to explain the extreme bendability of short DNA (Vafabakhsh & Ha, 2012). As a matter of fact, the difference between the length of a generic fiber and that of the natural curve becomes more and more apparent for short filaments, or for increasing values of the h/L ratio. Hence, assuming the neutral arc-length parametrization, the correct expression for the bending energy is the Eq. (20), while any other material fiber representation based on constant α requires the general expression (11). This contrasts with flexible polymers for which the concept of neutral curve loses importance and, even assuming the neutral arc-length parametrization (12), the energy is given by

$$\mathscr{E}_{\alpha_U} = \frac{bY}{2}\int_{s_m}^{s_M} ds\,\left\{ h\left[\left|\mathbf{t}_{\alpha_U}(s)\right| - 1\right]^2 - h^2\left[\frac{1}{2} - \alpha_U(s)\right]\frac{\left[\varphi'(s) - \Phi'(s)\right]^2}{\Phi'(s)} \right\}. \tag{26}$$

Finally, from a statistical mechanics point of view, at the equilibrium the Boltzmann distribution is $e^{-\frac{\mathscr{E}_{\alpha_U}}{k_BT}}$ rather than $e^{-\frac{\mathscr{E}_{WLC}}{k_BT}}$, weighting a statistical ensemble composed by polymers configurations satisfying the constrain of having constant neutral curve rather than constant line of centroids.

5.2. Numerical model for vesicles and polymers

Models for polymers, flexible films, membranes or vesicles often require a numerical implementation, in order to study shapes, fluctuations and dynamics, complementing the statistical mechanics analytical approach (Nelson, Piran, & Weinberg, 1989). These models in general consist of N impenetrable circular beads connected by links, arranged in a configuration which requires a well defined energy cost. A typical example is furnished by planar thermally fluctuating rings used as simplified models of fluctuating vesicles such as red blood cells. The Liebler-Singh-Fisher (LSF) model (Leibler, Singh, & Fisher, 1987), by instance, considers planar closed chains including the pressure and a curvature energy term such as $\sum_{i=1}^{N}\frac{k}{\Delta L}\left(1-\cos\Delta\varphi^{(i)}\right)$, where k is the constant bending modulus. Many aspect and variants of LSF have been discussed in the physics literature using a wealth of analytical and computational techniques (Camacho & Fisher, 1990; Camacho, Fisher, & Singh, 1991; Fisher, 1989; Gaspari, Rudnick, & Beldjenna, 1993; Haleva & Diamant, 2006; Landau, Lewis, & Schüttler, 2012; Levinson, 1992; Maggs, Leibler, Fisher, & Camacho, 1990; Mitra, Menon, & Rajesh, 2008), allowing the stretching of the ring (Marconi & Maritan, 1993; Romero, 1992), as well as a spontaneous curvature and locally varying bending modulus (Katifori et al., 2009).

In our theory the strain energy function (11) has been derived by a finite difference scheme, as the continuum limit of the sum of the blocks strain energy (1). Therefore, the discrete form of the Eq. (11) constitutes, without any further approximation, the appropriate expression to be used in numerical simulations (see Fig. 1B,B′ and SI). However, the fact that the uncoupling value of α_U in (8) depends crucially on the local value of the curvature of each block, makes it impossible to adopt a global neutral arc-length parametrization for discrete chains. This means that a discrete decoupled expression for the strain energy function is out of the question, because the discrete chain would result in a discontinuous polygonal, when N is finite (green dashed lines in Fig. 1B,B′). From an energetic point of view, there would be nothing wrong, as the energy would remain the same due to the strain energy invariance under a change of reference frame. However, from a graphical perspective, it would look awful! On the other side, adopting the constant α description yields the correct and more convenient expression for the numerical implementation of our model, valid for any value of N:

$$E_\alpha = \frac{Y}{2}\sum_{i=1}^{N}\Delta L_\alpha^{(i)}\left\{ F_\alpha^{(i)}\,\varepsilon_\alpha^{(i)2} + 2\frac{S_\alpha^{(i)}}{\Delta L_\alpha^{(i)}}\varepsilon_\alpha^{(i)}\left[\Delta\Phi^{(i)} - \Delta\varphi^{(i)}\right] + \frac{I_\alpha^{(i)}}{\Delta L_\alpha^{(i)2}}\left[\Delta\Phi^{(i)} - \Delta\varphi^{(i)}\right]^2 \right\}. \tag{27}$$

We emphasize that this expression holds for any elastic chain, be extensible or unextensible. The unextensibility condition should be enforced by keeping the lengths of the segments at the height $\alpha_U^{(i)}$ constants, in any conformational change, and modifying the representative α fiber accordingly. However, the detailed procedure of the numerical implementation of our model will be the subject of an upcoming publication.

5.3. Real filaments

Real biological filaments are characterized by local properties that can vary smoothly or abruptly along their contour. Our analysis focused on what we believe to be the most prominent property: the spontaneous curvature. However, geometric and mechanical properties may also characterize different portions of cellular filaments. In reality, filaments can only be considered homogeneous on average, with different heights (h) and depths (b) identifying each discrete protein-based segment. Simultaneously, the intrinsic mechanical properties of each monomer can differ, as in the case of the elastic modulus (Y), which we assumed to be constant in our analysis.

We believe that the entire framework assembled in this paper can be adapted to handle and accurately describe realistic biological filaments. The reasons lie in two main ingredients of our theory: the discrete scheme and the strain energy invariance under a change of reference frame. The finite difference scheme allows for a more precise description of biological shapes than any continuum theory, such as Cosserats' theory (Cosserat & Cosserat, 1909; Green et al., 1974a, 1974b; Naghdi & Rubin, 1984; Rubin, 2000) because any biological filament, whether it is a microtubule, actin, or intermediate filament, is ultimately composed of discrete units. Since the blocks are independent in our model, the geometrical and mechanical characteristics of biological filaments can be easily implemented locally, while preserving the general form of the strain energy as in (10). Furthermore, while the concept of material fibers becomes meaningless for non-homogeneous filaments, or at least non-parallel ones, the parametrization in terms of a reference segment $\alpha \in [0,1]$, inherent to any block, will always be possible, giving the concept of fiber a geometrical rather than material meaning. Most importantly, the existence of a neutral curve, allowing the axial-bending decoupled form of the strain energy, must remain valid in any context, highlighting once more the general value of our findings.

Declaration of competing interest

The authors declare that they have no known competing financial interests or personal relationships that could have appeared to influence the work reported in this paper.

Data availability

Data will be made available on request

Acknowledgments

We thank for the useful discussions, criticisms and suggestions Stefano Zapperi, Lev Truskinovsky, Silas Alben, Umut Orguz Salman and Daniel Rayneau-Kirkhope.

Appendix A. Supplementary data

Supplementary material related to this article can be found online at https://doi.org/10.1016/j.ijengsci.2023.103941.

References

Alberts, B. (2017). *Molecular Biology of the Cell*. Garland science.
Antman, S. (1968). General solutions for plane extensible elasticae having nonlinear stress-strain laws. *Quarterly of Applied Mathematics*, *26*(1), 35–47.
Atanackovic, T. (1998). Buckling of a compressible elastic ring. *Acta Mechanica*, *127*(1–4), 121–134.
Bausch, A., & Kroy, K. (2006). A bottom-up approach to cell mechanics. *Nature physics*, *2*(4), 231–238.
Bernoulli, J. (1691). Specimen alterum calculi differentialis in dimetienda spirali logarithmica, loxodromiis nautarum et areis triangulorum sphaericorum. Una cum additamento quodam ad problema funicularium, aliisque. *Acta Eruditorum, Junii*, 282–290.
Brangwynne, C. P., Koenderink, G. H., MacKintosh, F. C., & Weitz, D. A. (2008). Cytoplasmic diffusion: molecular motors mix it up. *The Journal of cell biology*, *183*(4), 583–587.
Camacho, C. J., & Fisher, M. E. (1990). Tunable fractal shapes in self-avoiding polygons and planar vesicles. *Physical Review Letters*, *65*(1), 9.
Camacho, C. J., Fisher, M. E., & Singh, R. R. (1991). Semiflexible planar polymeric loops. *Journal of Chemical Physics*, *94*(8), 5693–5700.
Chaskalovic, J., & Naili, S. (1995). Bifurcation theory applied to buckling states of a cylindrical shell. *Zeitschrift für angewandte Mathematik und Physik ZAMP*, *46*(1), 149–155.
Clebsch, R. F. A. (1862). *Theorie der elasticität fester körper*. BG Teubner.
Cosserat, E., & Cosserat, F. (1909). Théorie des corps déformables.
Coulomb, A. (1773). Essay on the application of the rules of maxima and minima to certain statics problems relavant to architecture. *Memoires presentes a l'Academie*, 343–384.
Doi, M., Edwards, S. F., & Edwards, S. F. (1988). *The theory of polymer dynamics, vol. 73*. oxford University Press.
Dorfman, K. D. (2018). The statistical segment length of DNA: Opportunities for biomechanical modeling in polymer physics and next-generation genomics. *Journal of Biomechanical Engineering*, *140*(2).
Euler, L. (1771). Genuina principia doctrinae de statu aequilibrii et motu corporum tam perfecte flesibilium quam elasticorum. *Novi Commentarii Academiae Scientiarum Petropolitanae*, 381–413.
Euler, L. (1960). *The rational mechanics of flexible or elastic bodies 1638-1788: introduction to vol. x and XI*. Springer Science & Business Media.
Fisher, M. E. (1989). Fractal and nonfractal shapes in two-dimensional vesicles. *Physica D: Nonlinear Phenomena*, *38*(1–3), 112–118.
Fixman, M., & Kovac, J. (1973). Polymer conformational statistics. III. Modified Gaussian models of stiff chains. *The Journal of Chemical Physics*, *58*(4), 1564–1568.
Fu, L., & Waas, A. (1995). Initial post-buckling behavior of thick rings under uniform external hydrostatic pressure.
Fuller, F. B. (1971). The writhing number of a space curve. *Proceedings of the National Academy of Sciences*, *68*(4), 815–819.
Gaspari, G., Rudnick, J., & Beldjenna, A. (1993). The shapes and sizes of two-dimensional pressurized self-intersecting rings, as models for two-dimensional vesicles. *Journal of Physics A: Mathematical and General*, *26*(1), 1.
Geggier, S., Kotlyar, A., & Vologodskii, A. (2011). Temperature dependence of DNA persistence length. *Nucleic Acids Research*, *39*(4), 1419–1426.
Ghosh, A., & Gov, N. (2014). Dynamics of active semiflexible polymers. *Biophysical Journal*, *107*(5), 1065–1073.
Green, A. E., Naghdi, P., & Wenner, M. (1974a). On the theory of rods. I. Derivations from the three-dimensional equations. *Proceedings of the Royal Society of London, Series A (Mathematical and Physical Sciences)*, *337*(1611), 451–483.
Green, A. E., Naghdi, P., & Wenner, M. (1974b). On the theory of rods II. Developments by direct approach. *Proceedings of the Royal Society of London, Series A (Mathematical and Physical Sciences)*, *337*(1611), 485–507.
Greenberg, J. M. (1967). On the equilibrium configurations of compressible slender bars. *Archive for Rational Mechanics and Analysis*, *27*(3), 181–194.
Haleva, E., & Diamant, H. (2006). Smoothening transition of a two-dimensional pressurized polymer ring. *The European Physical Journal E*, *19*, 461–469.
Harada, Y., Noguchi, A., Kishino, A., & Yanagida, T. (1987). Sliding movement of single actin filaments on one-headed myosin filaments. *Nature*, *326*(6115), 805–808.
Howard, J., & Clark, R. (2002). Mechanics of motor proteins and the cytoskeleton. *Applied Mechanics Reviews*, *55*(2), B39.
Kämmel, G. (1967). Der Einfluß der Längsdehnung auf die elastische Stabilität geschlossener Kreisringe. *Acta Mechanica*, *4*, 34–42.
Katifori, E., Alben, S., & Nelson, D. R. (2009). Collapse and folding of pressurized rings in two dimensions. *Physical Review E*, *79*(5), Article 056604.
Kirchhoff, G. (1859). Ueber das gleichgewicht und die bewegung eines unendlich dünnen elastischen stabes.. *Journal für die reine und angewandte Mathematik*, *1859*(56), 285–313.
Kosel, U. (1984). Biegelinie eines elastischen Ringes als Beispiel einer Verzweigungslösung. *ZAMM-Journal of Applied Mathematics and Mechanics/Zeitschrift für Angewandte Mathematik und Mechanik*, *64*(7), 316–319.
Kratky, O., & Porod, G. (1949). Röntgenuntersuchung gelöster fadenmoleküle. *Recueil des Travaux Chimiques des Pays-Bas*, *68*(12), 1106–1122.
Lagrange, J. L. (1853). *Mécanique analytique, vol. 1*. Mallet-Bachelier.
Lagrange, R., Jiménez, F. L., Terwagne, D., Brojan, M., & Reis, P. (2016). From wrinkling to global buckling of a ring on a curved substrate. *Journal of the Mechanics and Physics of Solids*, *89*, 77–95.
Landau, D. P., Lewis, S. P., & Schüttler, H.-B. (2012). *Computer simulation studies in condensed-matter physics XII: proceedings of the twelfth workshop, Athens, GA, USA, March 8-12, 1999, vol. 85*. Springer Science & Business Media.

Leibler, S., Singh, R. R., & Fisher, M. E. (1987). Thermodynamic behavior of two-dimensional vesicles. *Physical Review Letters*, *59*(18), 1989.
Levinson, E. (1992). Asphericity of two-dimensional closed pressurized random walks. *Physical Review A*, *45*(6), 3629.
Love, A. E. H. (2013). *A treatise on the mathematical theory of elasticity*. Cambridge University Press.
Maggs, A. C., Leibler, S., Fisher, M. E., & Camacho, C. J. (1990). Size of an inflated vesicle in two dimensions. *Physical Review A*, *42*(2), 691.
Magnusson, A., Ristinmaa, M., & Ljung, C. (2001). Behaviour of the extensible elastica solution. *International Journal of Solids and Structures*, *38*(46–47), 8441–8457.
Marconi, U. M. B., & Maritan, A. (1993). Deflated regime for pressurized ring polymers with long-range interactions. *Physical Review E*, *47*(5), 3795.
Marko, J. F., & Siggia, E. D. (1995). Stretching dna. *Macromolecules*, *28*(26), 8759–8770.
Martin, J., Davidson, E. C., Greco, C., Xu, W., Bannock, J. H., Agirre, A., et al. (2018). Temperature-dependence of persistence length affects phenomenological descriptions of aligning interactions in nematic semiconducting polymers. *Chemistry of Materials*, *30*(3), 748–761.
Michell, J. (1901). The theory of uniformly loaded beams. *The Quarterly Journal of Mathematics*, *32*, 28–42.
Mitra, M. K., Menon, G. I., & Rajesh, R. (2008). Phase transitions in pressurized semiflexible polymer rings. *Physical Review E*, *77*(4), Article 041802.
Naghdi, P., & Rubin, M. (1984). Constrained theories of rods. *Journal of Elasticity*, *14*(4), 343–361.
Nelson, D., Piran, T., & Weinberg, S. (1989). *Statistical mechanics of membranes and surfaces-proceedings of the 5th Jerusalem winter school for theoretical physics, vol. 5*. World Scientific.
Oshri, O., & Diamant, H. (2016). Properties of compressible elastica from relativistic analogy. *Soft matter*, *12*(3), 664–668.
Parent, A. (1713). De la veritable mecanique de resistance des solides. *Reflections sur la Systeme de M. Bernoulli de Bale Essais et recherches des Mathematiques et des physiques*, *3*, 187–201.
Romero, A. (1992). A simple model for shapes of vesicles in two dimensions. *Journal de Physique I (General Physics, Statistical Physics, Condensed Matter, Cross-Disciplinary Physics)*, *2*(1), 15–22.
Rubin, M. (2000). Cosserat theories: shells. Rods and Points.: Kluwer, the Netherlands.
Rubinstein, M., Colby, R. H., et al. (2003). *Polymer physics, vol. 23*. Oxford university press New York.
Schaller, V., Weber, C., Semmrich, C., Frey, E., & Bausch, A. R. (2010). Polar patterns of driven filaments. *Nature*, *467*(7311), 73–77.
Schamberger, B., Roschger, A., Ziege, R., Anselme, K., Amar, M. B., Bykowski, M., et al. (2022). Curvature in biological systems: its quantification, emergence and implications across the scales. *Advanced Materials*, Article 2206110.
Schmidt, R. (1996). Discussion:"initial post-buckling behavior of thick rings under uniform external hydrostatic pressure"(Fu, Lei and Waas, AM, 1995, ASME j. appl. Mech., 62, 338–345).
Schmidt, R., et al. (1979). A critical study of postbuckling analyses of uniformly compressed rings.
Schoen, I., Pruitt, B. L., & Vogel, V. (2013). The Yin-Yang of rigidity sensing: how forces and mechanical properties regulate the cellular response to materials. *Annual Review of Materials Research*, *43*, 589–618.
Seol, Y., Li, J., Nelson, P. C., Perkins, T. T., & Betterton, M. (2007). Elasticity of short DNA molecules: theory and experiment for contour lengths of 0.6–7 μm. *Biophysical Journal*, *93*(12), 4360–4373.
Tadjbakhsh, I. (1966). The variational theory of the plane motion of the extensible elastica. *International Journal of Engineering Science*, *4*(4), 433–450.
Tanaka, F., & Takahashi, H. (1985). Elastic theory of supercoiled DNA. *Journal of Chemical Physics*, *83*(11), 6017–6026.
Timoshenko, S. P. (1955). Strength of materials part 1. *Elementary theory and problems*, 165–310.
Timoshenko, S. (1983). *History of strength of materials: with a brief account of the history of theory of elasticity and theory of structures*. Courier Corporation.
Troger, H., & Steindl, A. (2012). *Nonlinear stability and bifurcation theory: an introduction for engineers and applied scientists*. Springer Science & Business Media.
Truesdell, C. (1984). The works of james Bernoulli (1973). In *An Idiot's fugitive essays on science* (pp. 202–208). Springer.
Truesdell, C., & Noll, W. (2004). The non-linear field theories of mechanics. In *The non-linear field theories of mechanics* (pp. 1–579). Springer.
Vafabakhsh, R., & Ha, T. (2012). Extreme bendability of DNA less than 100 base pairs long revealed by single-molecule cyclization. *Science*, *337*(6098), 1097–1101.
Vakakis, A., & Atanackovic, T. (1999). Buckling of an elastic ring forced by a periodic array of compressive loads. *Journal of Applied Mechanics, Transactions ASME*, *66*(2), 361–367.
Varshni, Y. (1970). Temperature dependence of the elastic constants. *Physical Review B*, *2*(10), 3952.
Yamakawa, H. (1977). Statistical mechanics of wormlike chains. In *Macromolecular chemistry–11* (pp. 135–141). Elsevier.